

Useful way to compensate for intrinsic birefringence caused by calcium fluoride in optical lithography systems

Zelong Zhou (周泽龙)^{1,2,*}, Hongbo Shang (尚红波)¹, Yongxin Sui (隋永新)¹,
and Huaijiang Yang (杨怀江)¹

¹Engineering Researcher Center of Extreme Precision Optics, Changchun Institute of Optics, Fine Mechanics and Physics, Chinese Academy of Sciences, Changchun 130033, China

²University of Chinese Academy of Sciences, Beijing 100049, China

*Corresponding author: zhouxm@163.com

Received October 11, 2017; accepted January 4, 2018; posted online March 6, 2018

Calcium fluoride is widely used in optical lithography lenses and causes retardation that cannot be ignored. However, few studies have been conducted to compensate for the retardation caused by calcium fluoride in optical lithography systems. In this Letter, a new index based on orientation Zernike polynomials is established to describe the value of retardation. Then, a method of retardation compensation is described. The method is implemented by clocking calcium fluoride lens elements, and the optimal rotation angles are calculated using a population-based stochastic optimization algorithm. Finally, an example is provided to validate the method.

OCIS codes: 220.3740, 260.1440, 260.5430.

doi: 10.3788/COL201816.032201.

Calcium fluoride is often used in the manufacture of lithography lenses because of its excellent ultraviolet transmittance, high laser durability, and achromatism. However, Burnett *et al.* reported that the intrinsic birefringence of calcium fluoride exceeds the tolerance level in the deep ultraviolet (DUV) range^[1]. Intrinsic birefringence causes a phase shift (i.e., retardation) between the s- and p-polarization components of rays that pass through an optical interface and, therefore, will reduce the imaging contrast of lithographic projection.

As one type of polarization aberration (PA), retardation is a physical quantity that has both magnitude and orientation. The magnitude reflects the size of the retardation, and the orientation reflects the direction of the fast axis; both can be obtained by singular-value decomposition (SVD)^[2]. On the basis of SVD, Ruoff and Totzeck further used orientation Zernike polynomials (OZP) to describe the polarization effects of retardation^[3]. The OZP terms can reflect the rotation symmetry of retardation, and the OZP coefficients represent the weights of various rotation symmetries.

PA, including retardation, has a significant effect on the imaging performance of optical lithography systems. Therefore, a compensation for retardation caused by calcium fluoride is considerably important. However, few studies have been conducted with regard to this aspect. A general compensation method was proposed by Serebriakov *et al.*^[4]. The phase retardation caused by intrinsic birefringence in DUV lithography was corrected by clocking several pairs of calcium fluoride lenses in different and special angles. This method can compensate for the retardation, but the rotation angles may not be optimal. On the basis of Ref. [4], we proposed a new method to

compensate for the retardation caused by intrinsic birefringence in lithography systems.

First, we establish a parameter that represents the effective value of retardation.

PA can be represented by a Jones matrix^[5], a 2×2 complex matrix that can be expressed as

$$J = \begin{pmatrix} j_{11} & j_{12} \\ j_{21} & j_{22} \end{pmatrix}. \quad (1)$$

By SVD, the polarization properties of lithography lenses can be expressed by five optical elements, i.e., a partial polarizer, a rotator, a retarder, a scalar phase, and a scalar transmission; thus, the Jones matrix J can be defined as^[2]

$$J = t e^{i\Phi} J_{\text{pol}}(d, \psi_p, \delta) J_{\text{rot}}(\alpha) J_{\text{ret}}(\phi, \psi_r), \quad (2)$$

where t represents the scalar transmission, and Φ represents the scalar phase; d , ψ_p , ϕ , and ψ_r represent the diattenuation value, bright axis direction, retardation value, and fast axis direction, respectively; δ represents the ellipticity of the partial polarizer, and α represents the rotation parameter. The retardation matrix J_{ret} in Eq. (2) can be expressed as

$$\begin{aligned} J_{\text{ret}}(\phi, \beta) &= \begin{pmatrix} \cos \phi - i \sin \phi \cos 2\beta & -i \sin \phi \sin 2\beta \\ -i \sin \phi \sin 2\beta & \cos \phi + i \sin \phi \cos 2\beta \end{pmatrix} \\ &= I \cos \phi - i \sin \phi \begin{pmatrix} \cos 2\beta & \sin 2\beta \\ \sin 2\beta & -\cos 2\beta \end{pmatrix}, \end{aligned} \quad (3)$$

where I is the 2×2 unit matrix. However, for optical lithography systems, $\sin \phi$ is quite small and can,

therefore, be approximated to ϕ . Then, we use OZP to decompose the retardation further:

$$\begin{aligned} J_{\text{ret}} I \cos \phi - i\phi \begin{pmatrix} \cos 2\beta & \sin 2\beta \\ \sin 2\beta & -\cos 2\beta \end{pmatrix} \\ = I \cos \phi - i \sum_{j=1}^{\infty} C_j \cdot OZ_j, \end{aligned} \quad (4)$$

where C_j is the OZP coefficient, and OZ_j is the OZP term, which is defined as

$$OZ_j = OZ_{n,\varepsilon}^m = R_n^m(\rho) O_\varepsilon^m(\theta) \quad (\varepsilon = 0, 1), \quad (5)$$

where $R_n^m(\rho)$ indicates the radial part, which is the same as the radial part of fringe Zernike polynomials. The angular part $O_\varepsilon^m(\theta)$ is defined as

$$\begin{aligned} O_0^m(\theta) &= \begin{pmatrix} \cos m\theta & \sin m\theta \\ \sin m\theta & -\cos m\theta \end{pmatrix}, \\ O_1^m(\theta) &= \begin{pmatrix} \sin m\theta & -\cos m\theta \\ -\cos m\theta & -\sin m\theta \end{pmatrix}. \end{aligned} \quad (6)$$

It is worth mentioning that three indices n , m , and ε can correspond to a certain index j . This correspondence was clearly discussed in a previous study^[6]. Table 1 shows the first 18 terms of OZP. In particular, when $m = 0$, the absolute value of the corresponding j is a square number.

We can easily obtain the orthogonality relation of OZP, which is given by

$$\begin{aligned} \frac{1}{2\pi(1+\delta_{m0})} \int_0^{2\pi} \int_0^1 (OZ_i \cdot OZ_j + OZ_j \cdot OZ_i) \rho \cdot d\rho \cdot d\theta \\ = \delta_{ij} I, \end{aligned} \quad (7)$$

where δ_{m0} and δ_{ij} are Kronecker delta functions.

When we use OZP to decompose the retardation matrix, we can obtain a series of OZP coefficients C_j . We wish to express the valid value of retardation by these coefficients. Intuitively, we propose the root-mean-square value fitted by OZP (RMSOZP). In statistics, the RMS value of a two-dimensional function $f(\theta, \rho)$ is defined as

$$R = \sqrt{\iint_{\theta,\rho} f^2(\theta, \rho) \cdot \rho \cdot d\rho \cdot d\theta}. \quad (8)$$

By this definition, we can obtain the RMSOZP of the retardation, which is given by

$$\begin{aligned} \mathfrak{R} &= \sqrt{\frac{1}{\pi} \int_0^{2\pi} \int_0^1 \left[\phi \begin{pmatrix} \cos 2\beta & \sin 2\beta \\ \sin 2\beta & -\cos 2\beta \end{pmatrix} \right]^2 \rho \cdot d\rho \cdot d\theta} \\ &= \sqrt{\frac{1}{\pi} \int_0^{2\pi} \int_0^1 \left(\sum_j C_j \cdot OZ_j \right)^2 \rho \cdot d\rho \cdot d\theta}. \end{aligned} \quad (9)$$

Using the orthogonality relation in Eq. (7), the RMSOZP \mathfrak{R} in Eq. (9) can be expressed as

$$\mathfrak{R} = \sqrt{\sum_j (2 - \delta_{m0}) C_j^2}. \quad (10)$$

Next, we will prove that the RMSOZP is equal to the RMS value obtained from Zernike decomposition. From

Table 1. First 18 terms of OZP

j	OZ_j	j	OZ_j	j	OZ_j
1	$\begin{pmatrix} 1 & 0 \\ 0 & -1 \end{pmatrix}$	4	$\sqrt{3}(2\rho^2 - 1) \begin{pmatrix} 1 & 0 \\ 0 & -1 \end{pmatrix}$	7	$\sqrt{8}(3\rho^3 - 2\rho) \begin{pmatrix} \cos \theta & \sin \theta \\ \sin \theta & -\cos \theta \end{pmatrix}$
-1	$\begin{pmatrix} 0 & 1 \\ 1 & 0 \end{pmatrix}$	-4	$\sqrt{3}(2\rho^2 - 1) \begin{pmatrix} 0 & 1 \\ 1 & 0 \end{pmatrix}$	-7	$\sqrt{8}(3\rho^3 - 2\rho) \begin{pmatrix} \cos \theta & -\sin \theta \\ -\sin \theta & -\cos \theta \end{pmatrix}$
2	$2\rho \begin{pmatrix} \cos \theta & \sin \theta \\ \sin \theta & -\cos \theta \end{pmatrix}$	5	$\sqrt{6}\rho^2 \begin{pmatrix} \cos 2\theta & \sin 2\theta \\ \sin 2\theta & -\cos 2\theta \end{pmatrix}$	8	$\sqrt{8}(3\rho^3 - 2\rho) \begin{pmatrix} \sin \theta & -\cos \theta \\ -\cos \theta & -\sin \theta \end{pmatrix}$
-2	$2\rho \begin{pmatrix} \cos \theta & -\sin \theta \\ -\sin \theta & -\cos \theta \end{pmatrix}$	-5	$\sqrt{6}\rho^2 \begin{pmatrix} \cos 2\theta & -\sin 2\theta \\ -\sin 2\theta & -\cos 2\theta \end{pmatrix}$	-8	$\sqrt{8}(3\rho^3 - 2\rho) \begin{pmatrix} \sin \theta & \cos \theta \\ \cos \theta & -\sin \theta \end{pmatrix}$
3	$2\rho \begin{pmatrix} \sin \theta & -\cos \theta \\ -\cos \theta & -\sin \theta \end{pmatrix}$	6	$\sqrt{6}\rho^2 \begin{pmatrix} \sin 2\theta & -\cos 2\theta \\ -\cos 2\theta & -\sin 2\theta \end{pmatrix}$	9	$\sqrt{5}(6\rho^4 - 6\rho^2 + 1) \begin{pmatrix} 1 & 0 \\ 0 & -1 \end{pmatrix}$
-3	$2\rho \begin{pmatrix} \sin \theta & \cos \theta \\ \cos \theta & -\sin \theta \end{pmatrix}$	-6	$\sqrt{6}\rho^2 \begin{pmatrix} \sin 2\theta & \cos 2\theta \\ \cos 2\theta & -\sin 2\theta \end{pmatrix}$	-9	$\sqrt{5}(6\rho^4 - 6\rho^2 + 1) \begin{pmatrix} 0 & 1 \\ 1 & 0 \end{pmatrix}$

the correspondence between the OZP and the scalar Zernike polynomials given by Ref. [6], we obtain

$$\begin{aligned}
& \phi \begin{pmatrix} \cos 2\beta & \sin 2\beta \\ \sin 2\beta & -\cos 2\beta \end{pmatrix} \\
&= \sum_j C_j \cdot OZ_j \\
&= \sum_{k=1}^{\infty} \left[C_{k^2} OZ_{k^2} + C_{-k^2} OZ_{-k^2} \right. \\
&\quad + \sum_{t=1}^k (C_{k^2+2t-1} OZ_{k^2+2t-1} + C_{k^2+2t} OZ_{k^2+2t} \\
&\quad + C_{-(k^2+2t-1)} OZ_{-(k^2+2t-1)} + C_{-(k^2+2t)} OZ_{-(k^2+2t)}) \left. \right] \\
&= \sum_{k=1}^{\infty} \left\{ C_{k^2} \begin{pmatrix} Z_{k^2} & 0 \\ 0 & -Z_{k^2} \end{pmatrix} + C_{-k^2} \begin{pmatrix} 0 & Z_{k^2} \\ Z_{k^2} & 0 \end{pmatrix} \right. \\
&\quad + \sum_{t=1}^k \left[C_{k^2+2t-1} \begin{pmatrix} Z_{k^2+2t-1} & Z_{k^2+2t} \\ Z_{k^2+2t} & -Z_{k^2+2t-1} \end{pmatrix} \right. \\
&\quad + C_{k^2+2t} \begin{pmatrix} Z_{k^2+2t} & -Z_{k^2+2t-1} \\ -Z_{k^2+2t-1} & -Z_{k^2+2t} \end{pmatrix} \\
&\quad + C_{-(k^2+2t-1)} \begin{pmatrix} Z_{k^2+2t-1} & -Z_{k^2+2t} \\ -Z_{k^2+2t} & -Z_{k^2+2t-1} \end{pmatrix} \\
&\quad \left. \left. + C_{-(k^2+2t)} \begin{pmatrix} Z_{k^2+2t} & Z_{k^2+2t-1} \\ Z_{k^2+2t-1} & -Z_{k^2+2t} \end{pmatrix} \right] \right\}, \quad (11)
\end{aligned}$$

where Z represents the scalar fringe Zernike polynomials. Using the relationship between the corresponding matrix elements in Eq. (11), we can directly get

$$\begin{aligned}
\phi \cos 2\beta &= \sum_{k=1}^{\infty} \left\{ C_{k^2} Z_{k^2} \right. \\
&\quad \left. + \sum_{t=1}^k [(C_{k^2+2t-1} + C_{-(k^2+2t-1)}) Z_{k^2+2t-1}] \right\}, \quad (12)
\end{aligned}$$

$$\begin{aligned}
\phi \sin 2\beta &= \sum_{k=1}^{\infty} \left\{ C_{-k^2} Z_{k^2} \right. \\
&\quad \left. + \sum_{t=1}^k [(C_{k^2+2t-1} - C_{-(k^2+2t-1)}) Z_{k^2+2t} \right. \\
&\quad \left. + (C_{-(k^2+2t)} - C_{k^2+2t}) Z_{k^2+2t-1}] \right\}. \quad (13)
\end{aligned}$$

According to the definition of RMS, the RMS values of $\phi \cos 2\beta$ and $\phi \sin 2\beta$ can be expressed as

$$\begin{aligned}
R_{\phi \cos 2\beta} &= \sqrt{\frac{1}{\pi} \int_0^{2\pi} \int_0^1 (\phi \cos 2\beta)^2 \rho \cdot d\rho \cdot d\theta} \\
&= \sqrt{\sum_{k=1}^{\infty} \left\{ C_{k^2}^2 + \sum_{t=1}^k [(C_{k^2+2t-1} + C_{-(k^2+2t-1)})^2] \right\}}, \quad (14)
\end{aligned}$$

$$\begin{aligned}
R_{\phi \sin 2\beta} &= \sqrt{\frac{1}{\pi} \int_0^{2\pi} \int_0^1 (\phi \sin 2\beta)^2 \rho \cdot d\rho \cdot d\theta} \\
&= \sqrt{\sum_{k=1}^{\infty} \left\{ C_{-k^2}^2 + \sum_{t=1}^k [(C_{k^2+2t-1} - C_{-(k^2+2t-1)})^2] \right\}}, \quad (15)
\end{aligned}$$

then,

$$\begin{aligned}
R_{\phi}^2 &= \frac{1}{\pi} \int_0^{2\pi} \int_0^1 \phi^2 \rho \cdot d\rho \cdot d\theta \\
&= \frac{1}{\pi} \int_0^{2\pi} \int_0^1 [(\phi \cos 2\beta)^2 + (\phi \sin 2\beta)^2] \rho \cdot d\rho \cdot d\theta \\
&= (R_{\phi \cos 2\beta})^2 + (R_{\phi \sin 2\beta})^2 \\
&= \sum_{k=1}^{\infty} \left[C_{k^2}^2 + C_{-k^2}^2 \right. \\
&\quad \left. + \sum_{t=1}^k (2C_{k^2+2t-1}^2 + 2C_{k^2+2t}^2 \right. \\
&\quad \left. + 2C_{-(k^2+2t-1)}^2 + 2C_{-(k^2+2t)}^2) \right] \\
&= \sqrt{\sum_j (2 - \delta_{m0}) C_j^2}. \quad (16)
\end{aligned}$$

Comparing Eq. (10) and Eq. (16), we find that

$$R_{\phi} = \mathfrak{R}. \quad (17)$$

Thus, the RMSOZP depends on the OZP coefficients and represents the effective value of the retardation. Moreover, the OZP terms correspond to the rotation symmetry properties of the system. Figure 1 shows the first 18 OZP terms arranged according to their symmetry properties. The colors are based on the radial dependence, and the short lines represent the direction of the eigen polarization state. The number M means M -fold rotation symmetry.

Assume that the retardation of an arbitrary lithography objective system is given by a series of OZ_j with coefficients C_j . We rotate several lenses, and the rotation angles are $\alpha_1, \alpha_2, \dots, \alpha_k$. After rotation, even though the RMSOZP of each single lens remains unchanged, the RMSOZP of the entire system is a function of these rotation angles:

$$\mathfrak{R} = F(\alpha_1, \alpha_2, \dots, \alpha_k).$$

Therefore, we can optimize the retardation by adjusting these rotation angles.

For this purpose, we use a population-based stochastic optimization (PSO) algorithm to seek the optimal rotation angles. PSO is originally attributed to Kennedy and Eberhart^[7]. Each possible solution is expressed as a particle, and each particle has its own position, velocity, and fitness. All the particles move around in the search space and arrive at the global optimum by updating current best known positions repeatedly. In addition, PSO has an uncomplicated structure, good convergence, and

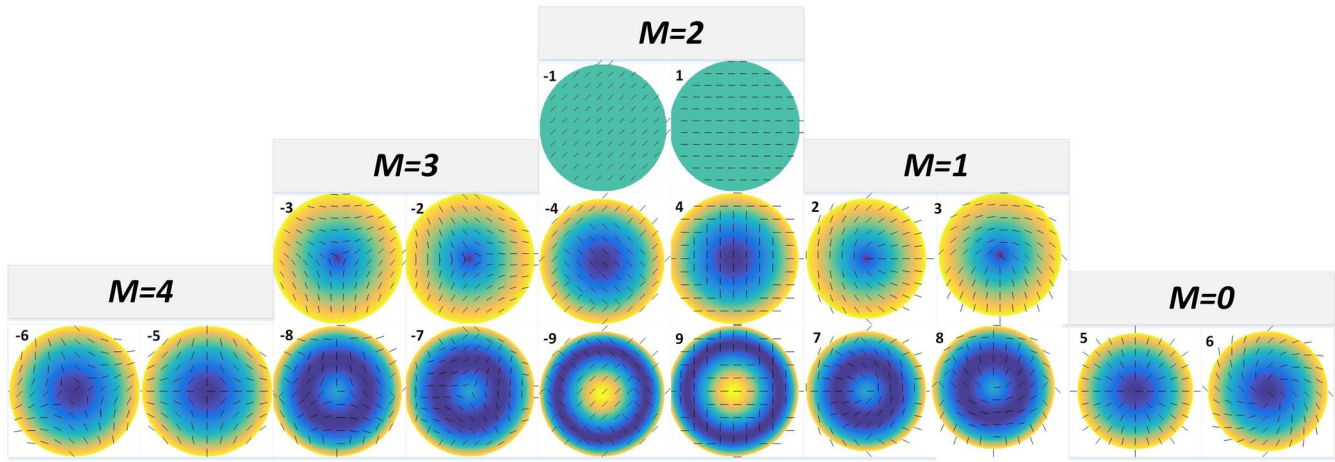


Fig. 1. OZP terms arranged according to the M -symmetry properties.

good stability. We call this method “PSO rotation” by applying PSO to the optimization of the lens rotation angles.

In PSO rotation, a set of rotation angles is treated as a particle’s position, and the corresponding RMSOZP of the retardation represents the particle’s fitness. The velocity of each particle is given by a mathematical formula.

The flow chart of PSO rotation is shown in Fig. 2.

To verify the effectiveness of PSO rotation, a patent lithographic lens was used to carry out this simulation experiment^[3]. Figure 3 shows the layout of the lithographic lens.

The numerical aperture (NA) is 0.75. The material of the 4th, 5th, 6th, 7th, 12th, 13th, 15th, and 16th lens

elements is calcium fluoride, and the material of the remaining lens elements is silica. It should be noted that only the eight calcium fluoride lens elements are rotated, and all the crystal axis orientations are along $\langle 111 \rangle$. The birefringence of calcium fluoride is -3.4 nm/cm^2 ^[2]. The central field was chosen for observation.

We choose all eight calcium fluoride lenses as rotation elements. PSO rotation can obtain the optimal eight rotation angles for the minimum RMSOZP of retardation by iteration. Figure 4 shows the convergence curve of the simulation.

The convergence curve shows that PSO rotation successfully reduces the retardation from 2.99 to 0.74 nm. The optimal rotation angles are shown in Table 2.

The comparison of the pupil maps of retardation before and after PSO rotation is shown in Fig. 5.

It is evident that the retardation at the edge of the pupil has been effectively compensated. Moreover, the retardation before and after the compensation has a three-fold rotation symmetry. This is consistent with the properties of calcium fluoride material in the $\langle 111 \rangle$ crystal

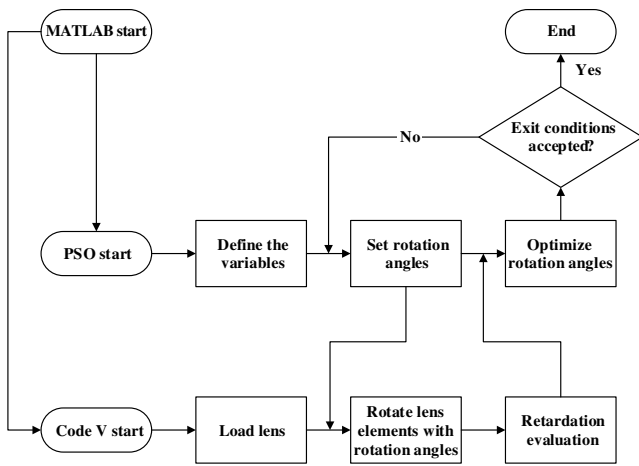


Fig. 2. Flow chart of PSO rotation.

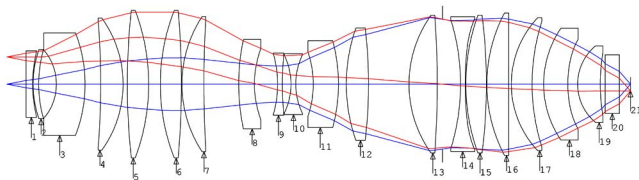


Fig. 3. Layout of a patent lithographic lens.

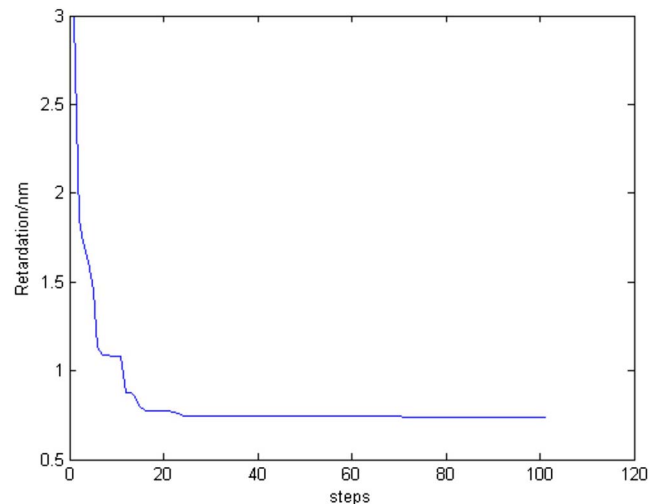


Fig. 4. Convergence curve of PSO rotation.

Table 2. Optimal Rotation Angles

Lens	4	5	6	7
Rotation angles (°)	344.8	311.8	40.8	97.8
Lens	12	13	15	16
Rotation angles (°)	36.2	213.5	0.8	271.5

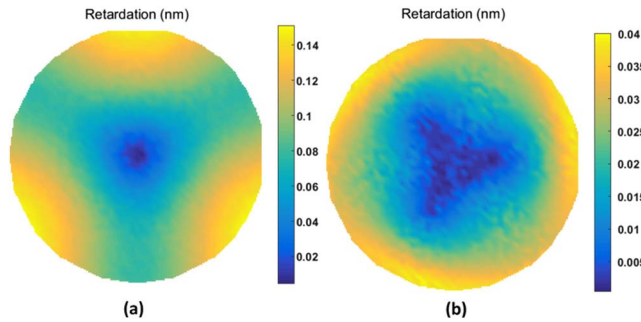


Fig. 5. Retardation pupil maps (a) before and (b) after PSO rotation.

orientation. To illustrate the rotation symmetry further, we compare the OZP coefficients before and after PSO rotation, as shown in Fig. 6.

It can be clearly seen from Fig. 6 that there are mainly four terms before PSO rotation: OZ_5 , OZ_{12} , OZ_{-3} , and OZ_{-8} . After PSO rotation, the coefficients of OZ_5 and OZ_{12} are almost invariable, but the coefficients of OZ_{-3} and OZ_{-8} are nearly zero. It means that the OZ_{-3} term and the OZ_{-8} term of retardation are greatly compensated for by PSO rotation. However, the OZ_5 term and the OZ_{12} term of retardation are rotation symmetric terms, so they remain unchanged after rotation.

It is worth pointing out that we can take one step further by considering the full field-of-view. We choose N fields-of-view (N is a positive integer). For each field-of-view, we can obtain an RMSOZP value. The RMS value of these RMSOZP values can be expressed as

$$\mathfrak{R}_{\text{RMS}} = \sqrt{\frac{\sum_{i=1}^N \mathfrak{R}_i^2}{N}}. \quad (18)$$

Then, we set $\mathfrak{R}_{\text{RMS}}$ as the fitness in the PSO algorithm. In this way, PSO rotation can compensate for the retardation from the central field to the edge field.

In conclusion, we propose a method called ‘‘PSO rotation,’’ which can effectively compensate for the retardation caused by the intrinsic birefringence of calcium fluoride in lithography systems. A simulated NA 0.75 lithographic lens was used to verify the PSO rotation. It is remarkable that we use the RMSOZP as an optimization objective. The RMSOZP can reveal both the effective value and rotation symmetry properties of the retardation. It should be stressed that in practical

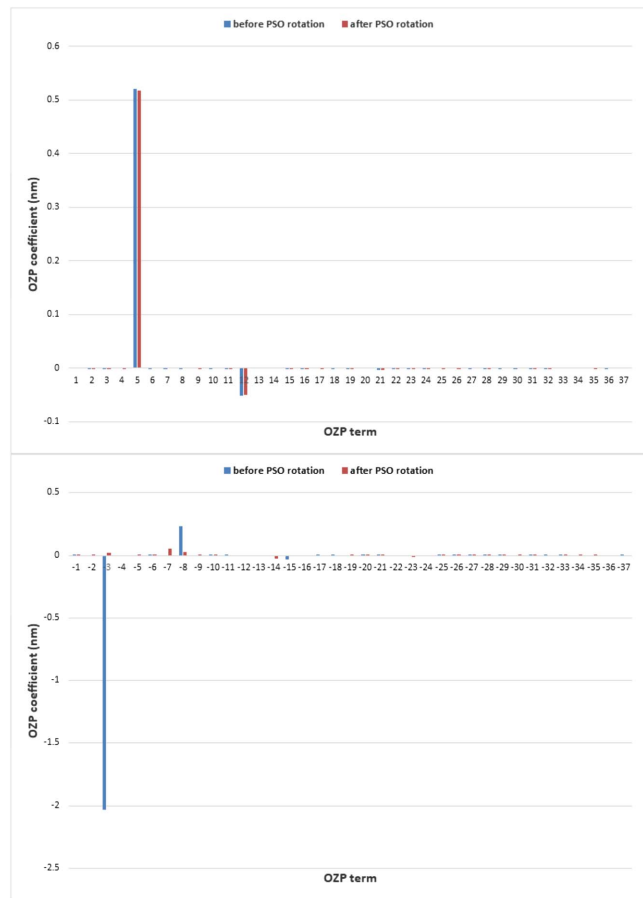


Fig. 6. OZP coefficients of retardation before and after PSO rotation.

engineering the rotation elements could be those lenses made from other materials, and retardation caused by stress birefringence can be taken into consideration. Hence, PSO rotation can be applied extensively in lithography systems.

References

1. J. H. Burnett, Z. H. Levine, E. L. Shirley, and J. H. Bruning, *J. Micro/Nanolithogr. MEMS MOEMS* **1**, 213 (2002).
2. B. Geh, J. Ruoff, J. Zimmermann, P. Gräupner, M. Totzeck, M. Mengel, U. Hempelmann, and E. Schmitt-Weaver, *Proc. SPIE* **6520**, 65200F (2007).
3. J. Ruoff and M. Totzeck, *Proc. SPIE* **7652**, 76521T (2010).
4. A. Serebriakov, F. Bociort, and J. Braat, *Proc. SPIE* **5754**, 1780 (2005).
5. R. C. Jones, *J. Opt. Soc. Am.* **31**, 488 (1941).
6. J. Ruoff and M. Totzeck, *J. Micro/Nanolithogr. MEMS MOEMS* **8**, 031404 (2009).
7. J. Kennedy and R. Eberhart, in *Proceedings of IEEE International Conference on Neural Networks*, Perth, Australia (1995), p. 1942.
8. Y. Omura, ‘‘Projection exposure methods and apparatus, and projection optical systems,’’ U.S. patent 6,864,961 (March 8, 2005).
9. J. H. Burnett, Z. H. Levine, and E. L. Shirley, *Phys. Rev. B* **64**, 241102 (2001).